GEOPHYSICAL RESEARCH LETTERS, VOL. 36, L16602, doi:10.1029/2009GL039216, 2009

Manifestation of the Pacific Decadal Oscillation in the Kuroshio

Magdalena Andres,[1,2] Jae-Hun Park,[1] Mark Wimbush,[1] Xiao-Hua Zhu,[3] Hirohiko Nakamura,[4] Kuh Kim,[5] and Kyung-Il Chang[5]

Received 16 May 2009; revised 17 July 2009; accepted 29 July 2009; published 28 August 2009.

[1] Pacific Decadal Oscillation (PDO) index is strongly correlated with vertically integrated transport carried by the Kuroshio through the East China Sea (ECS). Transport was determined from satellite altimetry calibrated with *in situ* data and its correlation with PDO index (0.76) is highest at zero lag. Total PDO-correlated transport variation carried by the ECS-Kuroshio and Ryukyu Current is about 4 Sv. In addition, PDO index is strongly negatively correlated, at zero lag, with NCEP wind-stress-curl over the central North Pacific at ECS latitudes. Sverdrup transport, calculated from wind-stress-curl anomalies, is consistent with the observed transport variations. Finally, PDO index and ECS-Kuroshio transport are each negatively correlated with Kuroshio Position Index in the Tokara Strait; this can be explained by a model in which Kuroshio path is steered by topography when transport is low and is inertially controlled when transport is high. **Citation:** Andres, M., J.-H. Park, M. Wimbush, X.-H. Zhu, H. Nakamura, K. Kim, and K.-I. Chang (2009), Manifestation of the Pacific Decadal Oscillation in the Kuroshio, *Geophys. Res. Lett.*, *36*, L16602, doi:10.1029/2009GL039216.

1. Introduction

[2] Interdecadal Pacific climate variability is reflected in the Pacific Decadal Oscillation (PDO) which can be represented with the PDO index, a measure of the state of sea surface temperature (SST) in the North Pacific [*Mantua et al.*, 1997]. *Miller et al.* [1998] and *Deser et al.* [1996] investigated the relationship between SST variability and changes in the ocean interior. Using historical hydrographic data, Deser et al. inferred decadal-scale variability in the strength of the Kuroshio Extension jet. Their inferred transport variations lagged wind-stress-curl variations by about 4–5 years, leading Deser et al. to suggest that Kuroshio Extension transport variations are a result of wind-driven changes in interior Sverdrup flow, with the response first carried to the western boundary by baroclinic Rossby waves and then advected to the Kuroshio Extension region by the western boundary current (WBC).

[3] *Qiu* [2003] also found evidence of low frequency modulation of Kuroshio Extension strength lagging PDO index by about 4–5 years. His analysis of satellite altimetry data indicated that the inferred transport variability is caused by the latitudinal dependence of baroclinic Rossby wave propagation of sea-surface-height (SSH) highs and lows excited by the winds in the eastern North Pacific. However, this model short-circuits the role of the Sverdrup transport and WBC advection suggested by *Deser et al.* [1996] since SSH anomalies propagate to the Kuroshio Extension directly from the east.

[4] *Seager et al.* [2001], using an ocean general circulation model, coupled with an atmospheric mixed layer model, suggested that SST variations in the central North Pacific result from an immediate response to wind due to advection of isotherms by Ekman drift, while SST variations in the Kuroshio Extension/Oyashio region are caused by a north-south shift of this confluence region which lags the wind variability by about 3 years.

[5] About 1500 km upstream of the Kuroshio Extension, in the East China Sea (ECS), sea level is negatively correlated with PDO index [*Han and Huang*, 2008], but the relationship between PDO index and Kuroshio transport in ECS has not yet been addressed. Here we investigate whether a PDO signal is apparent in ECS-Kuroshio transport, and whether this WBC's response to the wind is immediate (like that in the central North Pacific) or lagged (like that in the Kuroshio Extension). We present observational data, together with Sverdrup-transport calculations, which suggest that the WBC does have a PDO signal and that the response to winds over the central North Pacific is rapid, in contrast to the lagged response in the Kuroshio Extension. We also interpret observed WBC transport variations in terms of previous observations made in the ECS and the Japan/East Sea (JES).

2. Data

[6] PDO index, the time series of the first mode from empirical orthogonal function (EOF) analysis of Pacific sea surface temperature (SST) poleward of 20°N [*Mantua et al.*, 1997], is available from http://jisao.washington.edu/pdo/PDO.latest.

[7] In the subtropical North Pacific, WBC transport is carried by two branches which merge south of Japan [e.g., *Zhu et al.*, 2006]: the ECS-Kuroshio which flows through the ECS and the Ryukyu Current which flows along the south-eastern side of the Ryukyu Island chain (Figure 1). Vertically integrated transport of the ECS-Kuroshio near 28°N (KT) is available at 10-day interval through calibration of satellite altimetry data with net absolute transport determined using 13 months of *in situ* measurements from pressure-sensor-equipped inverted echo sounders (PIESs), ADCPs, current

[1]Graduate School of Oceanography, University of Rhode Island, Narragansett, Rhode Island, USA.
[2]Physical Oceanography Department, Woods Hole Oceanographic Institution, Woods Hole, Massachusetts, USA.
[3]State Key Laboratory of Satellite Ocean Dynamics, Second Institute of Oceanography, Hangzhou, China.
[4]Faculty of Fisheries, Kagoshima University, Kagoshima, Japan.
[5]Research Institute of Oceanography, School of Earth and Environmental Sciences, Seoul National University, Seoul, South Korea.

0094-8276/09/2009GL039216$05.00

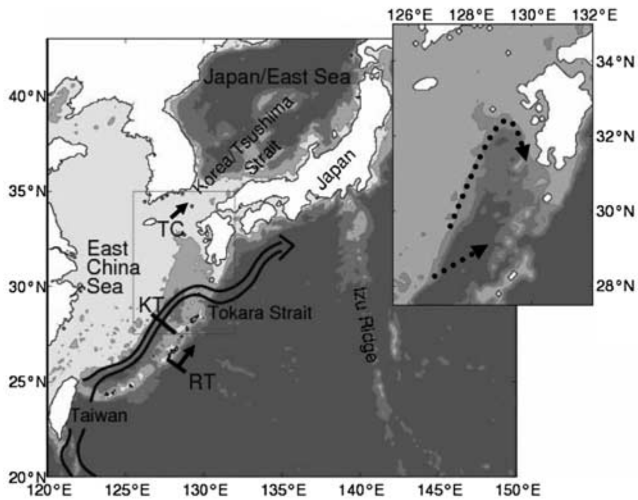

Figure 1. Circulation in the western North Pacific. ECS-Kuroshio mean-path, based on satellite altimetry, shown. ECS-Kuroshio and Ryukyu Current join downstream of the Tokara Strait. These transports were measured at the KT and RT lines, respectively. Downstream of the Izu Ridge, the WBC becomes a free jet: the Kuroshio Extension. In the ECS, the Tsushima Current (TC) flows into the JES through the Korea/Tsushima Strait. Inset shows topographically controlled and inertially controlled ECS-Kuroshio paths with contour lines at 200 m, 500 m, and 800 m depths.

meters, and hydrocasts [*Andres et al.*, 2008a, 2008b]. A similar vertically integrated transport time series has been determined for the Ryukyu Current near 26°N, RT [*Zhu et al.*, 2004]. While satellite altimetry data are related to surface transports through geostrophy, in each of these regions *in situ* measurements confirm that altimetry measurements are also approximately proportional to the vertically integrated absolute transport. These altimeter-determined transports are available starting in late 1992 when the TOPEX/Poseidon (later Jason-1) satellite began measurements.

[8] Kuroshio Position Index (KPI), which is a proxy for the north-south position of the ECS-Kuroshio as it exits the ECS through the Tokara strait [*Kawabe*, 2001], is calculated from daily sea-level data from 3 tide gages across the strait, corrected for the inverse barometer effect.

[9] The time series described above are shown in Figure 2. Each is averaged over one-year periods (January–December), resulting in 15-year long (1993–2007) yearly-mean time series except for RT, which is available through 2006 (Figures 2b–2e, solid circles). Correlation coefficients, *r*, of these time series with yearly-mean PDO index are listed in Table 1 together with the probability of zero correlation, *p,* calculated using 8 equivalent degrees of freedom (EDOF). EDOF was calculated from that time series which has the longest decorrelation time scale, namely, yearly-mean PDO index, as determined from the autocorrelation functions. In all cases, significant correlations with PDO index were found to be strongest at zero lag.

[10] National Center for Environmental Prediction (NCEP) provides wind-stress data at ~2° horizontal resolution and 6 hour interval [*Kalnay et al.*, 1996]. The data, available from www.ncep.noaa.gov, are used to calculate the

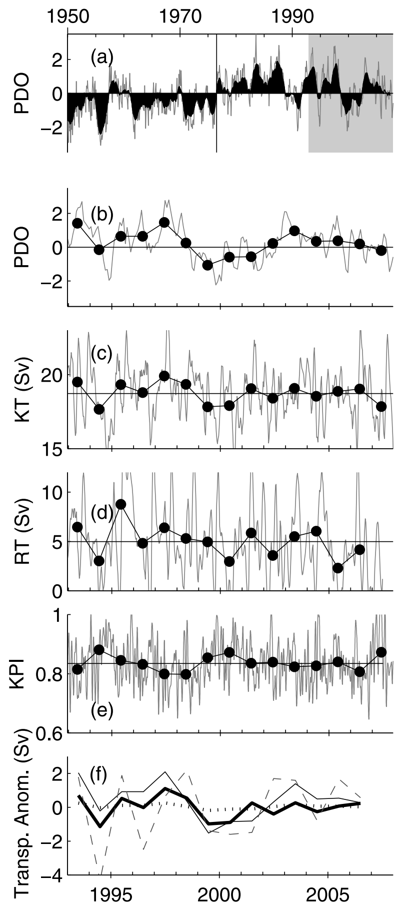

Figure 2. Time series of (a) monthly-mean PDO index, 1950–2007, with vertical line indicating the 1976/1977 regime shift and shaded area showing the time period plotted in the following panels, (b) monthly-mean PDO index, 1993–2007, (c) 10-day interval KT, (d) 10-day interval RT, (e) 30-day low pass-filtered KPI, and (f) annual mean Kuroshio transport anomalies as observed (heavy line) and calculated: T^{NP}_{PDO} (solid thin line), T^{NP}_{Total} (dashed line), and T^{PB}_{PDO} (dotted line). Solid circles in b–d represent yearly-means. Tick marks denote the beginnings of designated years.

wind-stress-curl field, $\nabla_H \times \vec{\tau}$, over the North Pacific from 1993 through 2006. The mean field is shown in Figure 3a.

3. Results and Discussion

3.1. Transport, PDO Index, and Wind-Stress-Curl

[11] Yearly-mean PDO index since 1993 is positively correlated with yearly-mean KT (at zero time-lag) at the

Table 1. Correlation (*r*) With Yearly-Mean PDO Index and Probability (*p*) of Zero Correlation

	r[a]	p
KT	0.76	0.01
RT	0.41	0.13
KT + RT	0.56	0.05
KPI	−0.66	0.05

[a]Yearly averages calculated with a window running from November to October (in order to catch a single PDO season with each average) lead to very similar correlation coefficients.

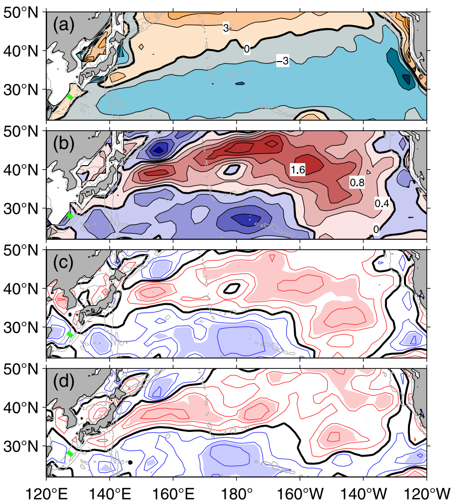

Figure 3. (a) Overall 1993 to 2006 mean $\nabla_H \times \vec{\tau}$. Contour interval is 3×10^{-8} N/m^3. Thick line shows zero contour. Values over water shallower than 100 m are masked. (b) Annual mean $\nabla_H \times \vec{\tau}$ regressed onto annual mean PDO index anomalies. Contour interval is 0.4×10^{-8} N/m^3. Correlations of annual mean $\nabla_H \times \vec{\tau}$ with (c) PDO index and (d) KT. Contour interval is 0.2 with the heavy line showing the zero contour. Regions with correlation significant at the 90% level (i.e., where $|r| \geq 0.45$) are shaded with significant negative correlations in blue and significant positive correlations in red. In all panels isobaths are shown at 500 and 3000 m depth with grey contours. KT line near 28°N is shown in green.

99% confidence level ($r = 0.76$). Linear regression shows that KT variation associated with PDO index changes is ~2 Sv. Total yearly-mean WBC transport (RT + KT) since 1993 also correlates positively with PDO index at zero lag ($r = 0.56$) and the associated combined WBC transport variation is ~4 Sv.

[12] This positive correlation between PDO index and WBC transport observed during the satellite record is also apparent in longer records. *Kawabe* [2001] derived estimates of ECS-Kuroshio transport from the early 1960s through 1995 from sea level difference across the Tokara Strait. The inferred transport was relatively low until the mid-1970s and higher through about 1990 with a ~2 Sv difference in mean transports during these periods [*Kawabe*, 2001, Figure 8]. Although not explicitly stated by Kawabe, the increase in mean transport was coincident with the 1976/1977 "regime shift" [e.g., *Nitta and Yamada*, 1989] during which PDO index increased markedly.

[13] To test whether the significant correlations observed between vertically integrated WBC transport and PDO index result from the ocean's response to the wind, we calculated correlations with $\nabla_H \times \vec{\tau}$. Correlation maps of yearly-mean $\nabla_H \times \vec{\tau}$ with PDO index (Figure 3c) and KT (Figure 3d) each show regions of significant negative correlation in the central North Pacific at ECS latitudes, reaching −0.82 for PDO index and −0.78 for KT. Notably, these correlations in the central North Pacific are higher than those in the Philippine Basin and ECS. In addition, correlations of PDO index and KT with wind-stress (as opposed to wind-stress-curl discussed above) in the Philippine Basin and ECS (not shown) are relatively low, implying that the primary forcing of interannual KT variability is remote rather than local.

[14] This suggests the following scenario. Enhanced westerly winds reduce central North Pacific SST, either by increased atmospheric heat transfer or by southward displacement of isotherms due to Ekman drift [e.g., *Seager et al.*, 2001]. This central Pacific cooling (together with warming off the American coast) is a signature of the PDO warm phase, when PDO index is positive. In addition to the central Pacific cooling, enhanced negative wind-stress-curl forces stronger southward Sverdrup flow [*Sverdrup*, 1947] in the subtropical North Pacific gyre. This is compensated by a stronger return flow in the ECS-Kuroshio (and Ryukyu Current, though the correlations with RT are not as strong).

[15] Since the ECS-Kuroshio response is rapid (i.e., <1 year) relative to interannual changes in the wind field (as demonstrated by lagged correlations), the Sverdrup relation,

$$Q_y = \frac{1}{\rho\beta}(\nabla_H \times \vec{\tau})', \tag{1}$$

can be used to determine a quasi-steady solution, in order to compare the magnitude of observed interannual KT variations to the expected wind-driven response, T (i.e., the Sverdrup transport). Here Q_y is the meridional volume transport anomaly per unit width (zonal), $(\nabla_H \times \vec{\tau})'$ is wind-stress-curl anomaly, ρ is density, and β is the variation of the Coriolis parameter with latitude. T is then determined by integrating equation (1) zonally along 24°N (the latitude at which the Kuroshio enters the ECS). Below we discuss various calculations of T, using different $(\nabla_H \times \vec{\tau})'$ in equation (1) and integrating over different zonal extents.

[16] First we isolate $(\nabla_H \times \vec{\tau}_{PDO})'$, that part of the total wind-stress-curl anomaly, $(\nabla_H \times \vec{\tau}_{Total})'$, which varies in conjunction with the PDO index, by regressing annual mean $(\nabla_H \times \vec{\tau}_{Total})'$ onto PDO index anomalies. The resulting spatial distribution (Figure 3b) is very similar to the first EOF of $(\nabla_H \times \vec{\tau}_{Total})'$ calculated by *Qiu* [2003]. Using $(\nabla_H \times \vec{\tau}_{PDO})'$, in equation (1) and integrating over the width of the entire North Pacific, we calculate T^{NP}_{PDO} (Figure 2e, solid thin line). T^{NP}_{PDO} agrees well with observed KT anomaly (Figure 2e, heavy line) with a root mean square (rms) difference of 0.8 Sv. (Note that T^{NP}_{PDO} has the same time evolution as PDO index, so the correlation between T^{NP}_{PDO} and KT is equal to that between PDO index and KT reported earlier.) For comparison, T^{NP}_{Total}, calculated using $(\nabla_H \times \vec{\tau}_{Total})'$, is shown (Figure 2e, dashed line). T^{NP}_{Total} differs, both in magnitude and shape, from observed KT, with an rms difference of 1.6 Sv. Also shown (dotted line) is T^{PB}_{PDO}, calculated with $(\nabla_H \times \vec{\tau}_{PDO})'$ integrated only over the Philippine Basin, i.e., west of the Izu Ridge. Clearly, this local forcing is not strong enough to induce the observed transport variations. $\nabla_H \times \vec{\tau}$ variations over the broad North Pacific cause flow variations which are communicated to the western boundary by Rossby waves. This communication is almost immediate for barotropic waves but slow for baroclinic waves. Hence, for the time-varying WBC-transport and integrated-wind-stress-curl fields, Sverdrup balance (equation (1)) applies only to the portion of the flow communicated by the barotropic Rossby waves. As a result, the calculated WBC transports do not correspond exactly to our measurements (Figure 2e).

[17] The correlations presented here in the WBC differ from observations ~1500 km downstream in the Kuroshio Extension where Kuroshio Extension strength lags PDO index by 4–5 years [e.g., *Qiu*, 2003]. Also, the magnitude of the PDO-related WBC transport variability presented here is only about half that in the Kuroshio Extension (~4 Sv compared to ~10 Sv). Nevertheless, since the total transport in the Kuroshio Extension is on the order of 100 Sv [e.g., *Howe et al.*, 2009], the ratio of PDO-related transport to total transport is similar in the WBC (~15%) to that in the Kuroshio Extension (~10%).

[18] At the latitude of the entrance to the ECS, 24°N, the first mode baroclinic Rossby waves take about 2.5–3 years to reach the western boundary from the central North Pacific [*Qiu*, 2003, Figure 7], much longer than the zero (<1 year) time-lag observed between KT and PDO index or KT and $\nabla_H \times \boldsymbol{\tau}$. Thus, it is unlikely that KT variations are a wind-driven response carried westward by baroclinic Rossby waves. This suggests that a linear description of the North Pacific is incomplete and inhomogeneities in the system (e.g., bottom topography, critical layers due to background flow, local wind forcing) are significant. The dynamics (in particular the role of barotropic Rossby waves) underlying the observed correlations remain to be investigated by models (e.g., quasi-geostrophic or primitive equation) that incorporate realistic topography, allow for non-linearity and linear damping of long Rossby waves, and are driven with idealized winds such as the first EOF mode of the wind-stress-curl field.

3.2. Marginal Seas and the PDO

[19] Correlation of yearly-mean PDO index with yearly-mean KPI is negative ($r = -0.66$) as is the correlation of yearly-mean KT with yearly-mean KPI ($r = -0.86$). These two correlations may result from competition between topographic and inertial steering of the Kuroshio jet as it exits the ECS through the Tokara Strait. *Sheremet* [2001] investigated the behavior of a WBC flowing past a boundary gap analytically, and found that potential vorticity conservation tends to make the current follow isobaths and hence loop into a gap, while inertia tends to make the current leap a gap. As can be seen in the inset in Figure 1, there is a kink in the isobaths along the ECS shelf-edge at about 28°N. The above noted correlations suggest that when the jet is inertially controlled (i.e., when KT is high), it continues in a straight path from this kink (towards the northeast), "jumps the gap" across the northern Okinawa Trough, and enters the Tokara Strait near its southern end (low KPI). On the other hand, when KT is relatively low, the jet is constrained to follow the topography, so it follows the shelf break (towards the north) and then "loops" anticyclonically along the isobaths towards the Tokara Strait, which it encounters at its northern end (high KPI). Physical parameters (e.g., gap-width, transport) in the ECS are similar to that part of the parameter-space in Sheremet's model in which transitions occur between the leaping and looping states. We also note that the analytical solution exhibits hysteresis in transitioning between these states.

[20] The correlations presented here and the mechanism described above are consistent with observations of negative correlation of PDO index with sea level in the JES [*Gordon and Giulivi*, 2004] and negative correlation of PDO index with sea level in the ECS [*Han and Huang*, 2008]. High sea level in the ECS corresponds with a relaxed thermocline across the Kuroshio and weaker transport. Under such conditions, the jet is topographically controlled and thus loops northward, leading to higher KPI. This may result in more water leaking into the JES through the Korea Strait. Thus the Tsushima Current may transport more subtropical waters into the JES resulting in warmer surface water, as observed by *Gordon and Giulivi* [2004], and therefore higher sea level in the JES.

4. Conclusions

[21] The use of *in situ* data to calibrate 15 years of satellite altimeter measurements with vertically integrated transport, has allowed us to establish that there is a positive correlation, at zero lag, between PDO index and KT in the ECS and, to a lesser extent, between PDO index and RT. This contrasts with results from the Kuroshio Extension region where the ocean's response lags changes in PDO index. These regional differences in lag are consistent with the modeling by *Seager et al.* [2001]. The expected interannual WBC transport variability calculated here, using NCEP winds and the Sverdrup relation, agrees well with the observed WBC transport variability. We also note that a primitive equation ocean model forced with wind stress and heat flux anomalies [*Miller et al.*, 1998] predicted a 10% change in gyre strength associated with the 1976/1977 regime shift. This is in agreement with our observations of the ECS-Kuroshio whose mean was ~19 Sv [*Andres et al.*, 2008a] and whose variability during the PDO-index changes over the last 15 years was ~2 Sv.

[22] While a dynamical explanation for the correlation between transport and PDO-index since 1993 remains to be investigated by numerical modeling, *Kawabe* [2001] successfully reproduced ECS-Kuroshio transport variations, including the marked mid-1970s increase, using a model of wind-driven Rossby waves in which observed variations in SSH along the Ryukyu Islands recorded by tide gages were caused mainly by the arrival of barotropic Rossby waves, and secondarily by first-baroclinic-mode Rossby waves.

[23] Finally, previously reported correlations between PDO index and SSH in the JES and the ECS are consistent with the correlations of KT and KPI with PDO reported here. These observations are well-explained by the model of a gap-leaping/topography-following jet in the northern Okinawa Trough.

[24] **Acknowledgments.** KPI records were kindly provided by Toru Yamashiro. MA, MW and JP were supported by ONR grant N000140210271. XZ was supported by the National Natural Science Foundation of China under grant 40776021 and the National Basic Research Programs of China under grant 2006CB400603. KK and KC were supported by the Korea EAST-I Program.

References

Andres, M., J.-H. Park, M. Wimbush, X.-H. Zhu, K.-I. Chang, and H. Ichikawa (2008a), Study of the Kuroshio/Ryukyu Current system based on satellite-altimeter and in situ data measurements, *J. Oceanogr.*, *64*, 937–950, doi:10.1007/s10872-008-0077-2.

Andres, M., M. Wimbush, J.-H. Park, K.-I. Chang, B.-H. Lim, D. R. Watts, H. Ichikawa, and W. J. Teague (2008b), Observations of Kuroshio flow variations in the East China Sea, *J. Geophys. Res.*, *113*, C05013, doi:10.1029/2007JC004200.

Deser, C., M. A. Alexander, and M. S. Timlin (1996), Upper ocean thermal variations in the North Pacific during 1970–1991, *J. Clim.*, *9*, 1840–1855, doi:10.1175/1520-0442(1996)009 < 1840:UOTVIT > 2.0.CO;2.

Gordon, A. L., and C. F. Giulivi (2004), Pacific decadal oscillation and sea level in the Japan/East Sea, *Deep Sea Res., Part I*, *51*, 653–663, doi:10.1016/j.dsr.2004.02.005.

Han, G., and W. Huang (2008), Pacific decadal oscillation and sea level variability in the Bohai, Yellow and East China Seas, *J. Phys. Oceanogr.*, *38*, 2772–2783, doi:10.1175/2008JPO3885.1.

Howe, P. J., K. A. Donohue, and D. R. Watts (2009), Stream-coordinate structure and variability of the Kuroshio Extension, *Deep Sea Res., Part I*, *56*, 1093–1116, doi:10.1016/j.dsr.2009.03.007.

Kalnay, E., et al. (1996), The NCEP/NCAR reanalysis 40-year project, *Bull. Am. Meteorol. Soc.*, *77*, 437–471, doi:10.1175/1520-0477(1996)077 < 0437:TNYRP > 2.0.CO;2.

Kawabe, M. (2001), Interannual variations of sea level at the Nansei Islands and volume transport of the Kuroshio due to wind changes, *J. Oceanogr.*, *57*, 189–205, doi:10.1023/A:1011195224933.

Mantua, N. J., S. R. Hare, Y. Zhang, J. M. Wallace, and R. C. Francis (1997), A Pacific interdecadal climate oscillation with impacts on salmon production, *Bull. Am. Meteorol. Soc.*, *78*, 1069–1079, doi:10.1175/1520-0477(1997)078 < 1069:APICOW > 2.0.CO;2.

Miller, A. J., D. Cayan, and W. B. White (1998), A westward-intensified decadal change in the North Pacific thermocline and gyre-scale circulation, *J. Clim.*, *11*, 3112–3127, doi:10.1175/1520-0442(1998)011 < 3112:AWIDCI > 2.0.CO;2.

Nitta, T., and S. Yamada (1989), Recent warming of tropical sea surface temperature and its relationship to the Northern Hemisphere circulation, *J. Meteorol. Soc. Jpn.*, *67*, 375–383.

Qiu, B. (2003), Kuroshio Extension variability and forcing of the Pacific Decadal Oscillations: Responses and potential feedback, *J. Phys. Oceanogr.*, *33*, 2465–2482.

Seager, R., Y. Kushnir, N. H. Naik, M. A. Cane, and J. Miller (2001), Wind-driven shifts in the latitude of the Kuroshio-Oyashio Extension and generation of SST anomalies on decadal timescales, *J. Clim.*, *14*, 4249–4265, doi:10.1175/1520-0442(2001)014 < 4249:WDSITL > 2.0.CO;2.

Sheremet, V. A. (2001), Hysteresis of a western boundary current leaping across a gap, *J. Phys. Oceanogr.*, *31*, 1247–1259, doi:10.1175/1520-0485(2001)031 < 1247:HOAWBC > 2.0.CO;2.

Sverdrup, H. U. (1947), Wind-driven currents in a baroclinic ocean; with application to the equatorial currents of the eastern Pacific, *Proc. Natl. Acad. Sci. U. S. A.*, *33*, 318–326, doi:10.1073/pnas.33.11.318.

Zhu, X.-H., H. Ichikawa, K. Ichikawa, and K. Takeuchi (2004), Volume transport variability southeast of Okinawa Island estimated from satellite altimeter data, *J. Oceanogr.*, *60*, 953–962, doi:10.1007/s10872-005-0004-8.

Zhu, X.-H., J.-H. Park, and I. Kaneko (2006), Velocity structures and transports of the Kuroshio and the Ryukyu Current during fall of 2000 estimated by an inverse technique, *J. Oceanogr.*, *62*, 587–596, doi:10.1007/s10872-006-0078-y.

M. Andres, Physical Oceanography Department, Woods Hole Oceanographic Institution, 266 Woods Hole Road, Woods Hole, MA 02543, USA. (mandres@whoi.edu)

K.-I. Chang and K. Kim, Research Institute of Oceanography/School of Earth and Environmental Sciences, Seoul National University, San 56-1, Shillim-dong, Gwanak-Gu, Seoul 151-742, South Korea.

H. Nakamura, Faculty of Fisheries, Kagoshima University, Shimoarata 4-50-20, Kagoshima 890-0056, Japan.

J.-H. Park and M. Wimbush, Graduate School of Oceanography, University of Rhode Island, 215 South Ferry Road, Narragansett, RI 02835, USA.

X.-H. Zhu, State Key Laboratory of Satellite Ocean Dynamics, Second Institute of Oceanography, 36 Bao-chu-bei Road, Hangzhou, Zhejiang 310012, China.